



**UNIVERSIDAD DE INVESTIGACIÓN DE
TECNOLOGÍA EXPERIMENTAL
YACHAY**

Escuela de Ciencias Físicas y Nanotecnología

**TÍTULO: Design, construction of a low-cost
hyperthermia equipment and validation
with Magnetic Nanoparticles**

Trabajo de integración curricular presentado como requisito para la obtención
del título de Ingeniería en Nanotecnología

Autor:

Jordy Steve Cevallos Benalcázar

Tutor:

PhD – Werner Bramer Escamilla

Co-tutor:

PhD – Sarah Briceño

Co-tutor:

PhD – Gema González Vázquez

Urcuquí, junio 2024

AUTORÍA

Yo, **Cevallos Benalcázar Jordy Steve**, con cédula de identidad 1726686023, declaro que las ideas, juicios, valoraciones, interpretaciones, consultas bibliográficas, definiciones y conceptualizaciones expuestas en el presente trabajo; así como, los procedimientos y herramientas utilizadas en la investigación, son de absoluta responsabilidad de el/la autora (a) del trabajo de integración curricular. Así mismo, me acojo a los reglamentos internos de la Universidad de Investigación de Tecnología Experimental Yachay.

Urququí, junio 2024.

Jordy Steve Cevallos Benalcázar
CI: 1726686023

AUTORIZACIÓN DE PUBLICACIÓN

Yo, **Cevallos Benalcázar Jordy Steve**, con cédula de identidad 1726686023, cedo a la Universidad de Investigación de Tecnología Experimental Yachay, los derechos de publicación de la presente obra, sin que deba haber un reconocimiento económico por este concepto. Declaro además que el texto del presente trabajo de titulación no podrá ser cedido a ninguna empresa editorial para su publicación u otros fines, sin contar previamente con la autorización escrita de la Universidad.

Asimismo, autorizo a la Universidad que realice la digitalización y publicación de este trabajo de integración curricular en el repositorio virtual, de conformidad a lo dispuesto en el Art. 144 de la Ley Orgánica de Educación Superior

Urcuquí, Junio 2024.

Jordy Steve Cevallos Benalcázar
CI: 1726686023

Resumen

En este proyecto de tesis, se diseñó y construyó un calentador de inducción de bajo costo para ayudar en el tratamiento de la hipertermia. Durante el proceso de construcción, el equipo fue sometido a meticulosos ajustes de diseño para cumplir con requisitos específicos. Los resultados mostraron que el equipo tenía una entrada de corriente alterna estable, oscilaciones de frecuencia estables en el rango de frecuencia media, lo cual es muy adecuado para el proceso de hipertermia, y un control de temperatura eficiente. Para validar el equipo, se mezclaron nanopartículas ferrimagnéticas y paramagnéticas (magnetita y hematita) con fluido corporal simulado para simular el fluido en un cuerpo vivo. El análisis de las curvas temperatura-tiempo de Nanopartículas Magnéticas (MNP) bajo la influencia del campo electromagnético generado por el calentador de inducción mostró aumentos de temperatura notables, demostrando la efectividad y confiabilidad del dispositivo para aplicaciones que involucran hipertermia. En general, esta investigación proporciona una forma económica de estudiar el efecto de las nanopartículas magnéticas sobre la hipertermia combinando nanopartículas magnéticas con tecnología de calentamiento por inducción. Al proporcionar calentamiento enfocado y no invasivo, el calentador de inducción recientemente diseñado y construido puede mejorar el estudio de un método alternativo para tratar el cáncer y presentar una opción competitiva a la costosa y compleja tecnología de hipertermia.

Palabras Clave:

Histéresis, Dominios magnéticos, Magnetización, Superparamagnética, Ferrimagnética.

Abstract

In this thesis project, a low-cost induction heater was designed and built to aid in treating hyperthermia. During the construction process, the equipment was subjected to meticulous design adjustments to meet specific requirements. The results showed that the equipment had stable alternating current input, stable frequency oscillations in the medium frequency range, which is very suitable for the hyperthermia process, and efficient temperature control. To validate the equipment, ferrimagnetic and paramagnetic nanoparticles (magnetite and hematite) were mixed with simulated body fluid to simulate the fluid in a living body. The analysis of the temperature-time curves of Magnetic Nanoparticles (MNPs) under the influence of the electromagnetic field generated by the induction heater showed notable temperature increases, proving the effectiveness and reliability of the device for applications involving hyperthermia. Overall, this research provides a low-cost way to study the effect of magnetic nanoparticles on hyperthermia by combining magnetic nanoparticles with induction heating technology. By providing focused, non-invasive heating, the recently designed and constructed induction heater can enhance the study of an alternative method to treat cancer and present a competitive option to expensive, complex hyperthermia technology.

Key Words:

Hysteresis, Magnetic domains, Magnetization, Superparamagnetic, Ferrimagnetic.

Contents

List of Figures	viii
List of Tables	ix
1 Introduction	1
1.1 Problem Statement	1
1.2 General and Specific Objectives	2
1.2.1 General Objectives	2
1.2.2 Specific Objectives	2
2 Theoretical Background	3
2.1 Cancer	3
2.2 Hyperthermia (HT)	4
2.2.1 Local Hyperthermia	4
2.2.2 Regional Hyperthermia	4
2.2.3 Whole Body Hyperthermia	4
2.3 Instruments used in hyperthermia treatments	4
2.3.1 Induction Heating System	5
2.3.2 Frequency and Power	5
2.3.3 Induction Solenoid/Coils	6
2.3.4 Thermocouples/Optical Probes for Temperature Measurements	7
2.3.5 Induction Heating Circuit and Device	7
2.4 Magnetothermal therapy	7
2.4.1 Magnetic Nanoparticles for Magnetothermal Therapy	7
2.4.2 Biocompatible MNPs used for hyperthermia	10
2.5 Characterization Techniques	11
2.5.1 X-rays Diffraction	11
2.5.2 Vibrating Sample Magnetometer (VSM)	12

3	Methodology	15
3.1	Construction of the Induction Heater	15
3.2	Synthesis of Magnetic Nanoparticles	16
3.2.1	Materials used in the synthesis	16
3.2.2	Synthesis Procedure	17
3.2.3	Characterization	17
3.3	Validation of the Induction Heating device by using the magnetite nanoparticles	19
4	Results & Discussion	21
4.1	Operation and Functionality of the Induction Heater System	21
4.2	Induction Heater Device Characteristics	21
4.3	Characterization of Magnetite Nanoparticles	24
4.3.1	X-rays Diffraction	24
4.3.2	Vibrating Sample Magnetometry	24
4.4	Validation of the induction heater with the MNPs	27
5	Conclusions & Outlook	29
	Bibliography	31

List of Figures

2.1	Induction Heating Circuit Diagram	8
2.2	Induction Heating Device	9
2.3	MNPs-mediated MHT for selective tumor cell destruction	10
2.4	Hysteresis Curve	13
3.1	Induction Heating Circuit Diagram	16
3.2	Protoboard Setup	17
3.3	Synthesis setup for MNPs	18
3.4	Experimental Setup of the Induction Heater and the MNPs	19
4.1	LC Circuit (Tank Circuit)	22
4.2	Final Setup of the Induction Heater	23
4.3	Final Setup of the Induction Heater with the Cooling System	23
4.4	Diffraction Spectres of the MNPs treated at different temperatures	25
4.5	Hysteresis loop pattern of MNPs treated ad different temperatures	26
4.6	MNPs comparison of temperature as a function of time	28

List of Tables

4.1	Magnetic properties of MNPs treated at different temperatures.	27
-----	--	----

Chapter 1

Introduction

Over the present century, cancer disease has been difficult to comprehend and is typified by the body's aberrant cells growing out of control. This may cause invasive harm to the organs and tissues nearby, possibly spreading to other parts of the body^{1,2}. Alterations in the DNA, chemical exposure, unhealthy lifestyle choices (like smoking and excessive drinking), and atmospheric factors (like pollution and radiation) can all lead to cancer². Lump formation, erratic bleeding, persistent coughing, loss of weight, and altered bowel habits are some of the symptoms. Patients with cancer also frequently experience pain, nausea, sleep difficulties, persistent tiredness, and despair. Magnetic field-based or magnetothermal therapy using magnetic nanoparticles shows potential as a powerful alternative to standard cancer treatments³. It offers accurate drug delivery with minimal side effects and has been proven to stop cell division, induce apoptosis, regulate the immune system, and halt angiogenesis and metastasis³. This emerging therapy holds promise for treating various types of cancer.

Devices for treating hyperthermia frequently utilized in cancer therapy include radio-frequency (RF) systems, microwave antennas, and RF antennas. These devices are used to control the heat in cancerous tissues by raising their temperatures to 40 – 43°C and combining them with radiotherapy or chemotherapy^{4,5}. Deep-seated tumors are heated using radio-frequency antennas that operate between 70 and 150 MHz⁶. The cancer treatment is treated by The purpose of MW antennas, which run at 434–2450 MHz, is to heat superficial malignancies⁷. In this work, a low-cost hyperthermia device will be designed and constructed, and its effectiveness will be validated using magnetic nanoparticles, which can react to an external magnetic field by some mechanisms, such as Neel relaxation or Brownian relaxation and Eddy's current heating effect⁸⁻¹¹. Then, by taking advantage of that mechanism, the generation of heat can be obtained and used to reach the temperature needed for hyperthermia treatment.

1.1 Problem Statement

Heating by electromagnetic induction is used as a method to generate heat in conductor materials. Hence, the field of hyperthermia treatment has promised to improve cancer therapy results, but carrying out this procedure uses equipment that is expensive and not widely accessible. This research aims to construct a low-cost hyperthermia

device using the induction heating principle, prioritizing affordability, effectiveness, and simplicity. Magnetic nanoparticles are used for testing the heating capacity of the equipment.

1.2 General and Specific Objectives

1.2.1 General Objectives

Construction of affordable magnetothermic equipment based on induction heating.

1.2.2 Specific Objectives

1. Design a low-cost magnetothermic equipment based on the literature.
2. Design of the electric circuit of the induction heater.
3. Validation of circuit performance.
4. Construction of the induction coil and cooling system.
5. Synthesize magnetic nanoparticles.
6. Characterize the magnetic nanoparticles.
7. Validation of the induction heater with the magnetic nanoparticles.

Chapter 2

Theoretical Background

2.1 Cancer

In the last decade, the battle against many diseases has been a problem, but cancer is one of the most formidable challenges to comprehend since it is required to understand in depth the body's intricate mechanisms. Cancer is the uncontrollable growth of cells that are not normal in the body, this abrupt growth can lead to an invasion in the surrounding tissues and as a consequence the spreading to other parts of the body, this event can damage or even destroy organs making the functioning of the body abnormal^{1,2}. Carcinoma, adenocarcinoma, sarcoma, lymphoma/leukemia, and myeloma are the origin to determine what type of cancer is present in the system^{12,13}. Genetic alterations, exposure to certain chemicals and toxins, lifestyle choices like smoking and excessive drinking, and exposure to radiation and pollution are some variables that can contribute to the development of cancer². Lumps, irregular bleeding, frequent coughing, unusual weight loss, and changes in bowel movements are the symptoms of cancer¹⁴. Various symptoms, such as pain, exhaustion, insomnia, sadness, and nausea, are commonly experienced by people with cancer^{15,16}.

Nowadays, a powerful alternative to standard treatments for cancer therapy has emerged, which is magnetic field-based or magnetothermal therapy, due to its good efficacy and fewer side effects. Magnetic nanoparticles (MNPs) are being studied and monitored for cancer diagnosis and therapy^{17,18}. Some advantages that MNPs can have are the load with chemotherapeutic drugs and antibodies and the capacity to be delivered to tumor tissue using an external magnetic field¹⁹. It has been proved that magnetic fields stop cell division, produce apoptosis, control the immune system, and stop angiogenesis and metastasis³. Hence, with its accurate drug delivery and the minimal side effects, magnetothermal therapy which uses magnetic nanoparticles—provide a promising alternative to treat the various type of cancer.

2.2 Hyperthermia (HT)

Hyperthermia (HT) is a treatment technique that can be used for therapeutic procedures in cancer by raising the cell's temperature around the tumor zone. This technique can be used in conjunction with other cancer treatments. Depending on the procedure that is being carried out the different types of hyperthermia can be applied²⁰.

2.2.1 Local Hyperthermia

Local hyperthermia is a procedure that heats a tumor site. The heat can be generated using different methods, such as ultrasound, radiofrequency energy, microwave energy, or magnetic fields. Local hyperthermia aims to raise the temperature of the tumor to 41-45 °C, which can weak, harm, or eliminate cancer cells²⁰.

2.2.2 Regional Hyperthermia

Regional hyperthermia involves heating a specific body part to high temperatures to target tumors. There are three main methods: intrinsic, thermal, and constant hyperthermic peritoneal perfusion (CHPP). Intrinsic hyperthermia applies heat to tumors using applicators, while thermal hyperthermia heats larger body areas by circulating heated fluids. CHPP targets peritoneal cancers by infusing a heated chemotherapy agent into the abdominal cavity, raising the tissue temperature to 41-42 °C. This technique is typically used to treat advanced tumors in areas like the thighs, abdomen, or pelvis.²⁰.

2.2.3 Whole Body Hyperthermia

Whole-body hyperthermia (WBH) involves raising the temperature of the entire body to at least 41 °C to treat various conditions, including cancer. WBH can be achieved using either radiation heat or extracorporeal technologies. Immersion in a hot water bath and radiant heat with ultraviolet (UV) radiation are the usual techniques utilized for WBH. In extracorporeal WBH, A blood circuit is formed next to the body, creating an extracorporeal ring. The blood is heated by passing through a hot air or water bath before being infused into the main vein. WBH treatment sessions typically last four hours, with two hours to reach the target temperature, one hour to maintain it, and one hour to cool down. WBH has the potential to provide the most uniform heat delivery, but it also carries the greatest risk of complications, including elevated temperatures in the brain, liver, heart, or lungs²⁰.

2.3 Instruments used in hyperthermia treatments

Hyperthermia treatments use a variety of frequencies to apply heat to tumors, including microwaves ranging from 433 to 2450 MHz, radio waves ranging from 100 KHz to 150 MHz, and ultrasound at frequencies of 0.2-5 MHz. The choice of frequency depends on the depth and location of the tumor, with radio frequencies at 8-12 MHz being optimal for deep-seated tumors and microwave heating at 434-915 MHz being best for superficial tumors²⁰. In addition to these methods, hot water perfusion, resisting wire embeds, ferromagnetic seeds, nanoparticles, and

infrared radiators can also be used to deliver heat. Two types of probes are used in hyperthermia treatments: an applicator to transmit energy to the tissue and a temperature probe to monitor tissue temperature. To ensure that the required temperature is achieved without damaging healthy tissue, the temperature of the tumor and adjacent tissues is monitored throughout the procedure, to maintain local temperatures below 44°C and whole body temperature below 42°C. To improve the precision of heat-delivery, ultrasound or MRI can be used to position heat-delivery devices, and new types of nanoparticles that are less toxic to nearby tissues are being developed as absorbers^{20,21}.

2.3.1 Induction Heating System

Induction heating system uses electromagnetic induction to heat an electrically conductive material, consisting of an induction power supply, an induction coil, and a work-piece. An alternating current generated by the power supply is passed through the induction coil, which creates a magnetic field around the workpiece, inducing electrical currents and generating heat within the workpiece. The flow of electric current starts when the object is placed in the magnetic field, and this flow of current produces heat because of the object's resistance to the flow of electricity, also called eddy current.^{8,9} Induction heating involves the use a varying magnetic field created by a high-frequency alternating current that provokes the eddy current withing the object⁹. These systems are widely used in applications such as brazing, annealing, hardening, melting, and forging and are particularly useful when fast, precise, and localized heating is required. Moreover, induction heating systems are energy-efficient and environmentally friendly, producing heat only where needed, without wasting energy on heating the surrounding environment. They can be customized to fit the specific needs of each application, with various sizes and shapes of induction coils available and designed to operate at different frequencies and power levels²².

2.3.2 Frequency and Power

Induction heating is a process that uses the principle of electromagnetic induction to generate heat in a conductive material. Therefore, the frequency of the time-variable magnetic field produced by alternating the voltage has the same frequency as the current in the induction heating coil²³. There is three ranges of frequencies: low frequency (up to 10 kHz), medium frequency (10 kHz and 70 kHz), and high frequency (above 70 kHz). The frequency in induction heating is crucial as it affects the penetration depth; the higher the frequency, the lower the penetration depth. This means that different frequencies are used depending on the desired heating application²³. On the other hand, the power affects the temperature of the object being heated, in simple words, higher power levels result in faster temperature rise^{23,24}. In addition, depending on the frequency of the electromagnetic waves emitted there will be a ionizing radiation (IR) which is potentially harmful since it uses high energy particles and also non ionizing radiation (NIR) which carries less energies that are not lethal²⁵. The frequencies ranges are 10 – 10¹⁶ Hz for NIR and 10¹⁶ Hz and above for IR²⁶.

2.3.3 Induction Solenoid/Coils

Induction coils have several applications, such as magnetic particle heating and induction heating. In magnetic particle heating, an electromagnetic induction coil is used to heat the object with a medium-high frequency while the magnetic field is alternating²⁷. In induction heating, the coil generates the alternating magnetic field to generate heat in the conductive material²⁷. Therefore, Induction coils are essential in induction heating devices as they generate the magnetic field to heat the object. The geometry of the coil influences how the magnetic field is generated and distributed around the object^{28,29}. Also, the geometry affects the inductance cause it is related to the turns³⁰. The magnetic field (B) and the inductance (L) of the coil can be calculated by using the following equations:

$$B = \mu \cdot N \cdot I \quad (2.1)$$

$$L = \frac{N^2 \cdot \mu_0 \cdot A}{l} \quad (2.2)$$

or Air Cored Inductor coil

$$L = \frac{0.393 \cdot N^2 \cdot r^2}{9r + 10l} \quad (2.3)$$

Where:

- B is the magnetic field strength.
- L is the inductance
- μ is the permeability of the material.
- μ_0 is the material's permeability inside the coil.
- N is the number of turns in the coil.
- I is the current flowing through the coil.
- A is the cross-sectional area of the coil.
- l is the length of the coil
- r is the radius of the coil

Additionally, the resonant frequency in induction heating is related to the coil design and parameters such as the number of turns, diameter, and spacing of windings. The resonant frequency can be obtained using the following equation³¹:

$$f = \frac{1}{2\pi \sqrt{LC}} \quad (2.4)$$

The resonant frequency equation is obtained by solving the differential equation that is related to the LC circuit behavior.

The coil size used for NP-MIH is determined by the tumor size or area to be treated. Different coils can be used for magnetic hyperthermia, including solenoid, Helmholtz, birdcage, and pancake coils. Cooling the solenoid is necessary when magnetic field intensities exceed 20 mT to prevent adverse effects on hyperthermia. Insulated coils and low thermal conductivity materials are used to achieve thermal equilibrium between the sample and coil at an optimal temperature^{32,33}.

2.3.4 Thermocouples/Optical Probes for Temperature Measurements

The thermometric components of magnetic hyperthermic equipment must be sensitive, accurate, and non-invasive to ensure the desired therapeutic effect is achieved without adversely affecting healthy tissue. Sophisticated thermometric systems like MRI, IR thermography, and optical fiber thermometry can solve this problem^{32,33}.

2.3.5 Induction Heating Circuit and Device

An induction heating device presents a viable option for magnetothermal therapy reaching the hyperthermia temperature, a medical condition where heat destroys cancerous cells in the human body. A detailed schematic of the circuit for an induction heating system is available for review in Figure 2.1, providing insight into the underlying technology that makes this treatment possible. Additionally, a completed and fully operational induction heating device can also be observed in Figure 2.2, serving as a testament to the practicality and effectiveness of this treatment option.

2.4 Magnetothermal therapy

Magnetothermal therapy is a highly potential technique that can be used to treat some diseases, such as cancer and neurodegenerative disorders. This therapy involves using an external magnetic field that affects magnetic nanoparticles. As the response, it generates heat, which can then be applied to cause hyperthermia, target and destroy cancer cells specifically, or stimulate brain neurons. Numerous investigations have looked into the various uses of magnetothermal therapy. A magnetothermal method was created by Liu and partners to effectively mark stem cells for in vivo monitoring and targeted stroke therapy³⁶. Dai et al have demonstrated that magnetothermal therapy can be efficient by manipulating cell signaling by sensitizing breast cancer cells³⁷. Superparamagnetic ferrofluids were created by Leonel et al. for use in hyperthermia applications, and they demonstrated improved cell-killing capabilities in magnetic hyperthermia experiments³⁸. The results of these studies show the diversity of therapeutic applications that magnetothermal therapy can be applied for.

2.4.1 Magnetic Nanoparticles for Magnetothermal Therapy

Magnetic nanoparticles are increasingly being explored as a tool for magnetothermal therapy (hyperthermia treatments), which involve heating a part of the body or the whole body to high temperatures for medical purposes, including cancer treatment. Local hyperthermia, regional hyperthermia, and whole body hyperthermia are the three types of hyperthermia that can be used in conjunction with magnetic nanoparticles to achieve therapeutic effects. By

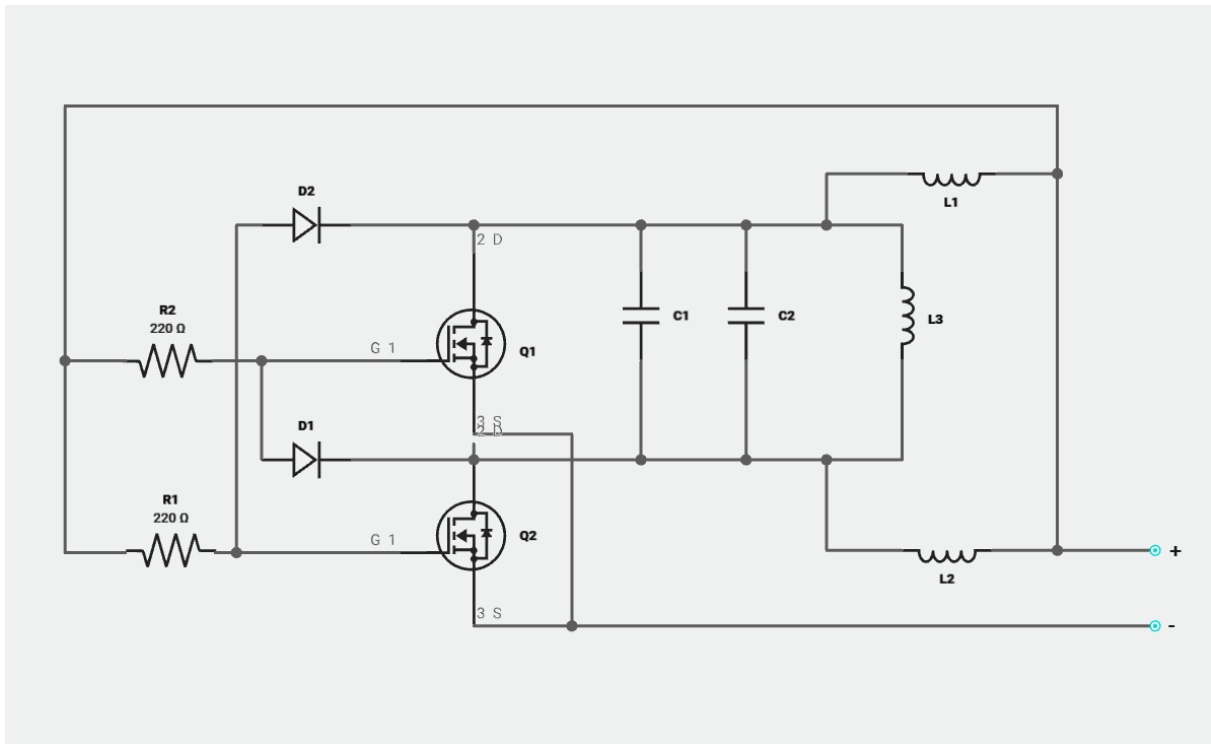


Figure 2.1: Induction Heating Circuit Diagram (Based on³⁴)

utilizing the magnetic properties of nanoparticles, they can be directed to specific areas of the body and heat can be generated locally in a controlled manner, leading to more efficient and effective hyperthermia treatments^{20,21,32,33,39}.

Over the years, magnetic nanoparticles have gained a lot of interest due to their potential and unique properties that can be used in a wide range of applications. Besides, magnetic nanoparticles present magnetic properties but also a small size and high surface area to volume ratio. Nanoparticles have shown great potential in various fields but magnetic nanoparticles specifically have been studied demonstrating good applications in biotechnology, environmental remediation, drug delivery and also imaging⁴⁰.

Magnetic nanoparticles can be potentially used in therapy and in nanomedicine for treating and diagnosing disease^{41,42}. Due to they can be used as contrast agents, they can be used for magnetic resonance imaging (MRI) to provide anatomical information⁴¹. Moreover, MNPs can be functionalized to actively target specific areas within the body allowing therapeutic applications. This application makes the MNPs excellent candidates for tumor targeting and medical imaging⁴¹. In addition, MNPs are used to heat cells in specific zones of the body to about 42 – 45°C which is the hyperthermia range by using an external magnetic field, this heating can treat diseases helping to kill cancer cells⁴³ There are various mechanisms in which magnetic nanoparticles can be heated up in an alternating magnetic field. One of those mechanisms is called Brownian losses, where MNPs behave like tiny magnets constantly

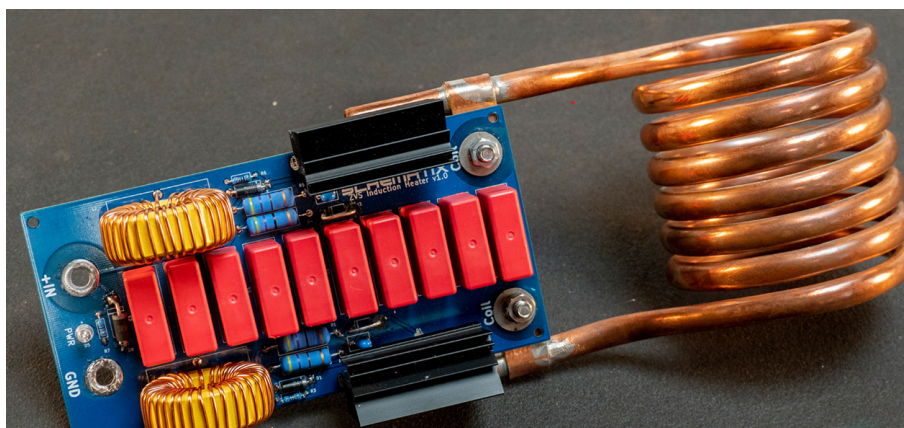


Figure 2.2: Induction Heating Device (Taken from³⁵)

rotating and moving due to the interaction with the fluid¹⁰. Another mechanism is the Néel relaxation losses, where MNPs magnetic moments rapidly change their orientation in response to the external magnetic field¹¹. Moreover, hysteresis losses that is related to the hysteresis phenomenon occurs when ferromagnetic material is involved. When the magnetic field is taken off from the ferromagnetic material the energy does not completely go back to the system⁴⁴. In addition, eddy current occurs in ferromagnetic metal nanoparticles, and it is generated when the MNPs are exposed to an alternating magnetic field that produces a resistivity in the material, making it increase its temperature similar to a resistance^{45,46}. The heating of the nanoparticles occurs because there is a short thermal relaxation time constants⁴⁷. By controlling the concentration, size, and properties of the medium, it can be optimized the efficiency of heating MNPs, that is, the Specific absorption rate (SAR)⁴⁸⁻⁵¹.

According to Rajan et al. and Behrouzki et al. in their works related to hyperthermia treatments^{20,39}, explains how the use of magnetic nanoparticles (MNPs) combined with heat can be used for thermal treatment, particularly for metastatic and locally advanced disease stages that cannot be treated with surgery. This technique involves infusing iron oxide nanoparticles into the target tissue and heating them with a magnetic field. The method is useful for heating tumors located deep in the body, such as in the skull or pelvis. The size and depth of the tumor affect the homogeneous delivery of heat as in Figure 2.3.

Previous hyperthermia techniques have had limitations, such as being unable to target heat to the tumor, difficulties in achieving a homogeneous distribution of heat, and challenges in targeting indiscernible micrometastases. Ferro-, ferri-, and super ferromagnetic materials, such as Fe/MgO, are appropriate for this treatment method due to their biocompatibility^{20,21,39}.

According to Rajan et al. and Behrouzki et al. in their works related to hyperthermia treatments^{20,39}, the different types of magnetic materials, including ferro- and ferrimagnetic materials, which have natural alignment of atomic magnetic dipole moments in a specified direction. In bulk materials, these materials have multidomains, but when reduced in size to the nanometer-scale level, the domain region transitions from multidomain to a single domain. Single-domain magnetic nanoparticles exhibit two important types of magnetism: single-domain ferromagnetic

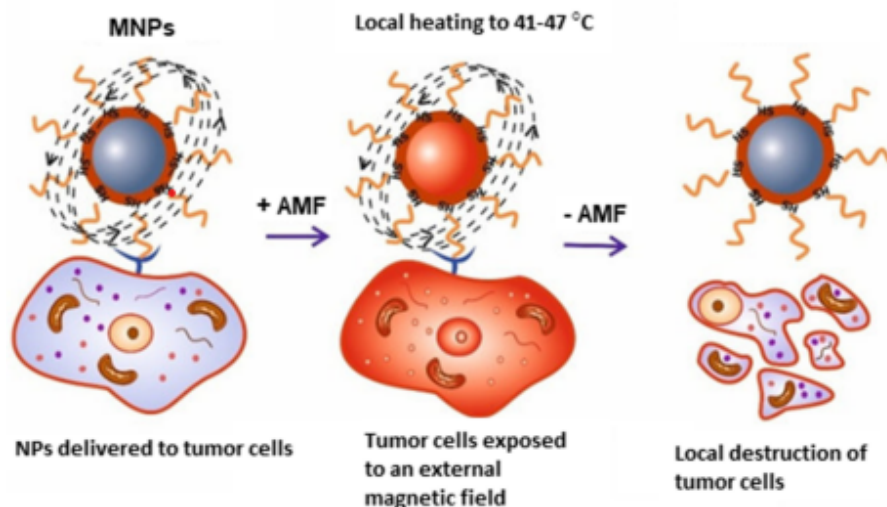


Figure 2.3: MNPs-mediated MHT for selective tumor cell destruction (Taken from³⁹)

nanoparticles and single-domain superparamagnetic nanoparticles^{20,39}.

The size of the magnetic nanoparticles strongly influences their coercivity, which impacts their magnetic nature. As the size of the particles decreases from multidomain zones to single domain zones, the coercivity increases, where it reaches a maximum, and finally decreases, remaining zero at the superparamagnetic transition point. Superparamagnetic nanoparticles have high saturation magnetization when a field is applied, and they lose their magnetism completely when the field is removed at thermal equilibrium. These particles are useful for biomedical applications as they prevent aggregation and reduce the risks associated with thrombus formation. Additionally, their size within the superparamagnetic limit at biologically tolerated magnetic fields dissipates sufficient heating power, making them useful for magnetic hyperthermia applications^{20,39}.

2.4.2 Biocompatible MNPs used for hyperthermia

MNPs with biocompatible and biodegradable properties and suitable functionalized surfaces are important materials for magnetic hyperthermia (MHT). MNPs made of iron, cobalt, nickel, manganese, zinc, gadolinium, magnesium, their alloys, and oxides, such as CoFe_2O_4 , NiFe_2O_4 , ZnFe_2O_4 , CuFe_2O_4 , MnFe_2O_4 , Gd-doped Zn-Mn, Fe-doped Au, and Zn-Mn-doped iron oxides, have been explored for MHT due to their superior magnetic properties. Iron oxide nanoparticles (IONPs) are the most researched biocompatible MNP for MHT and have been licensed by the US Food and Drug Administration and the European Medicines Agency for clinical applications. Both magnetite and maghemite phases of iron oxides are good choices because they have better biodegradable nature, chemical stability, and lower toxicity³⁹.

The magnetic properties of superparamagnetic (SPM) iron oxide NPs produce the high magnetization nature of bulk magnetite with the paramagnetic nature of iron ions ($\text{Fe}^{3+}/\text{Fe}^{2+}$). The natural property of SPM IONPs of high saturation magnetic and magnetization sensitivity under the applied magnetic field, and losing its magnetization completely by removing of the field, can be effectively utilized for MHT applications. Other Fe-based alloys, such as Fe-Pt and Fe-Co, have also been explored for MHT, with Fe-Pt alloys gaining attention for their stable magnetic properties for heat generation. Anisotropic-structured magnetic Janus NPs with distinct physical and chemical properties, such as Fe_3O_4 -Pd, PMMA/ Fe_3O_4 /PAA, and carbon-coated Fe-Co, have also been utilized for synergistic chemo-thermal/photothermal/magneto-thermal therapy and have shown high therapeutic results and minimal side effects, making them suitable for combined therapies³⁹.

Magnetic nanoparticles have been studied with significant attention because they allow a new point of view for cancer treatment by using the hyperthermia temperature range. Targeting cancer cells with a higher precision and reaching deep tissues can be obtained with a non-invasive treatment, magnetic hyperthermia. Magnetic nanoparticles not only include other anti-tumor agents but also can be placed at the tumor site⁵². Nanoparticles such as magnetite are commonly used in biomedicine because they are compatible with the human body. There are clinical studies suggests that magnetite nanoparticles are safe for biomedical applications as reported in the Hyperthermia Treatment Planning article⁵³ They have a high level of magnetization which allows them to be strongly attracted by magnetic fields. Furthermore, magnetite nanoparticles have a large surface area, and they are chemically stable, which allows them to easily be modified for different uses in medicine⁵⁴. Magnetic hyperthermia is used to heat and damage tumor cells in a zone using magnetic nanoparticles such as magnetite. These nanoparticles are heated up by controlling an external magnetic field. Therefore, it allows the healthy tissue to be unharmed by specifically targeting the cancer cells^{52,55}.

Magnetic nanoparticle-induced hyperthermia (NP-MIH) is a localized heating treatment (magnetothermal therapy) for tumors utilizing the properties of an alternating magnetic field induced in one of the following ways mentioned above^{32,33}

2.5 Characterization Techniques

2.5.1 X-rays Diffraction

X-rays were discovered by Röntgen in 1895. He found that X-rays have wavelengths between 10 and 0.01 nanometers (nm) and are defined as electromagnetic waves that use high energy. X-ray diffraction (XRD) is a powerful non-destructive method that is used to study the structure of crystalline materials by analyzing the diffraction pattern generated at certain angles of the atomic plane of the crystal lattice when a monochromatic X-ray beam is scattered⁵⁶⁻⁵⁹. This diffraction pattern or diffractogram provides information about the crystalline structure, phases, crystal orientation, grain size, crystallinity, tension and crystal defects, all these information that is provided by the diffractogram is like a fingerprint of the atomic arrangements^{57,58,60}.

William Henry Bragg and William Lawrence Bragg in 1913 explained how X-rays is diffracted when they hit a crystal by the Bragg law. Atoms in crystals are arranged in three-dimensional grids that resemble X-ray wavelengths,

resulting in diffraction that is comparable to light passing through slits⁵⁶. According to Bragg's theory, X-rays interact with atoms in crystal layers to form a pattern known as crystal planes. These crystal planes are patterns formed by the interaction of the flat waves and the layers of atoms in a crystal. The relation between the distance between the crystal planes d_{hkl} , the angle of incidence θ , the diffraction order (n) and the X-ray wavelength λ is defined by the following equation⁵⁶:

$$n\lambda = 2d_{hkl} \sin \theta_1 \quad (2.5)$$

On the other hand, the grain size can be estimated by using the Scherrer Equation:

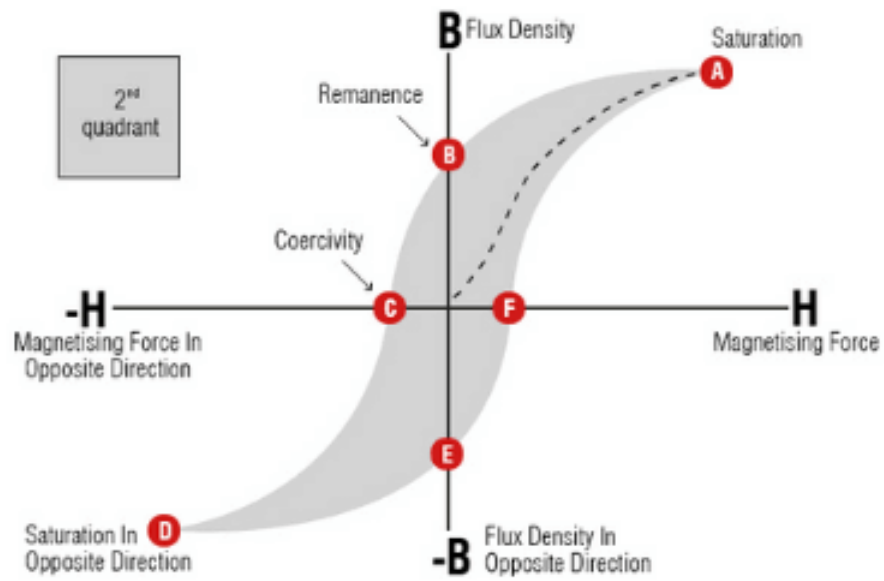
$$D = \frac{K\lambda}{\beta \cos(\theta_2)} \quad (2.6)$$

Where:

- D is the average crystallite size
- K is the Scherrer constant (depends on the material analyzed)
- λ is the wavelength of the X-ray radiation used
- β is the full width at half maximum (FWHM) of the diffraction peak in radians
- θ_1 is the Bragg angle related to the crystalline lattice.
- θ_2 diffraction angle from the XRD peaks are related to the crystalline structure of the material.

2.5.2 Vibrating Sample Magnetometer (VSM)

Measuring the magnetic properties of materials is possible by using a vibrating sample magnetometer (VSM) machine. The VSM allows the study of materials because it can work in specific conditions, this machine can work at high temperatures in gas-controlled environments⁶¹. Measurements in magnetic hysteresis in thin films can be improved by modifying the design and calibration of the VSM⁶² and hysteresis loops for rock magnetism can be analyzed by using software tools⁶³. In addition, VSM can be used to study the type of magnetic domain present in environmental samples, such as sediments in rivers⁶⁴. The relationship between the magnetizing force and the induced magnetic flux density is shown by a hysteresis loop⁴⁴. Ferromagnetic materials lose heat in an alternating magnetic field because to hysteresis loss⁴⁴. Additionally, a detailed hysteresis curve can be observed in the Figure 2.4.

Figure 2.4: Hysteresis Curve (Taken from⁶⁵)

Chapter 3

Methodology

3.1 Construction of the Induction Heater

To construct the induction heater several steps were done to guarantee the proper design, implementation and ensure the correct operation of the device by some tests.

The circuit design shown in Figure 3.1 was initially created using an existing schematic of an induction heater, with adjustments according to the required needs. The materials used to build the induction heater were the following:

- 2x IRFP260N MOSFETs.
- 2x fast diodes.
- 10k resistors.
- 2x 470ohm - 2w resistors.
- 2x inductors with 25 turns of 1mm² wire around yellow toroidal cores.
- 10x 0.63 μ F capacitors.
- 12V - 4A power source.
- Wood.
- 3 bakelites.
- Coil work (6 turns, 3.8 cm diameter, coil length 4.0 cm).

The prototype of the circuit was built in a protoboard (figure 3.2) to verify the oscillation using a 12V - 4A by using an oscilloscope. Then, the circuit was transferred onto the final base, the bakelites. The bakelite circuits

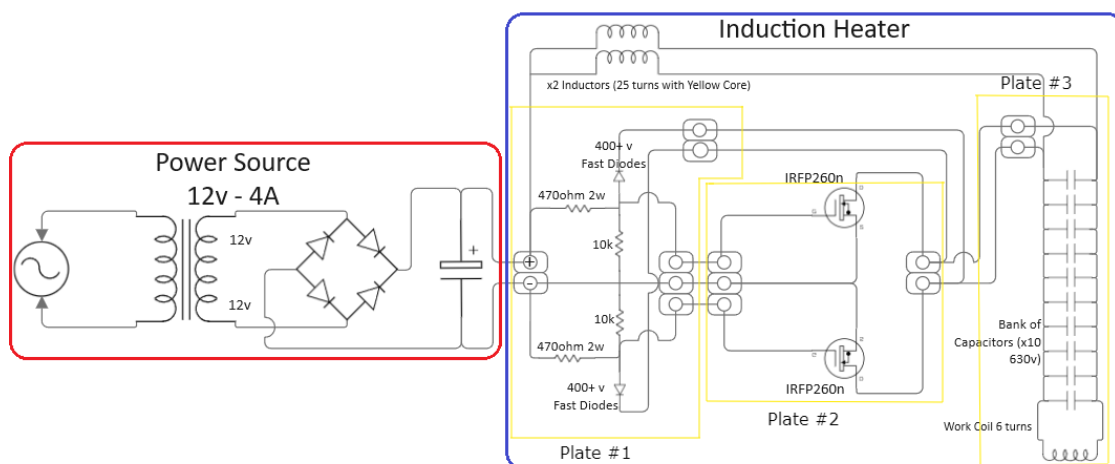


Figure 3.1: Induction Heating Circuit Diagram (Based on⁶⁷)

was previously designed by using the PCB Wizard Software⁶⁶ and printed by using a CNC machine model CNC3-3018Pro. After this final implementation, another test was carried out to confirm that the circuit oscillate correctly at the final base. To regulate the temperature of the device, a cooling system was integrated (Figure 3.4), and its efficacy was assessed through a thermal test carried out with the equipment for 2 hours. During this process, the alternating current, temperature, and oscillation were monitored by using an ammeter, thermocouples, and oscilloscope, respectively. Finally, a final test was done to see if the device worked by using a piece of metal and looking if this piece was heated up.

3.2 Synthesis of Magnetic Nanoparticles

Synthesis of the magnetic nanoparticles of magnetite (Fe_3O_4) was carried out by using a precipitation method described by Berger et al. in their work Preparation and Properties of an Aqueous Ferrofluid⁶⁸.

3.2.1 Materials used in the synthesis

1. 1 g of $\text{FeCl}_2 \cdot 4\text{H}_2\text{O}$.
2. 2,7 g of $\text{FeCl}_3 \cdot 6\text{H}_2\text{O}$.
3. 25 mL of distilled water.
4. 0,5 g of NaOH in 5 mL of distilled water.

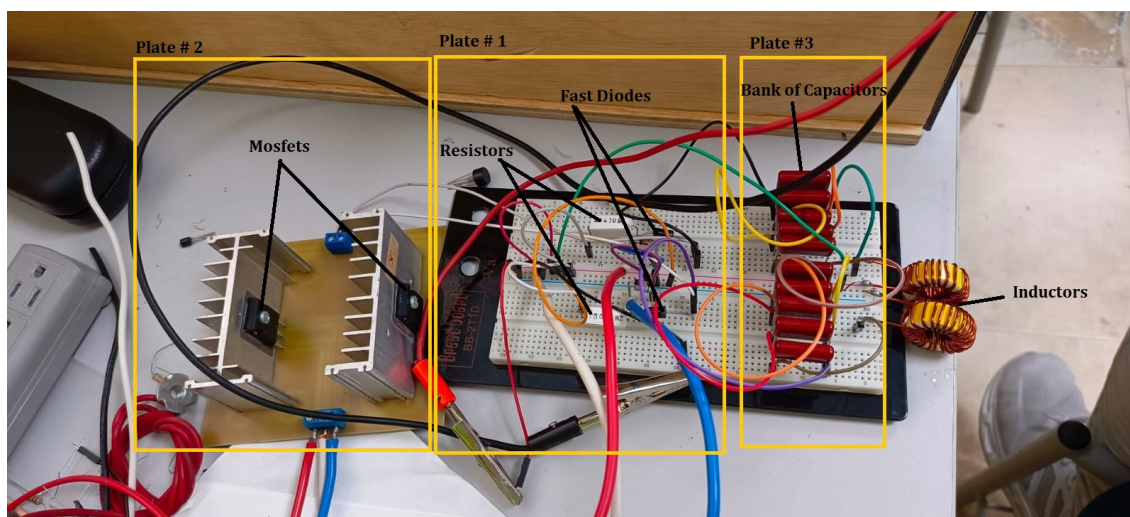
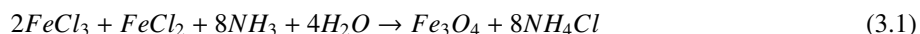


Figure 3.2: Protoboard Setup

3.2.2 Synthesis Procedure

The synthesis process consists of the combination of 2.7 grams of FeCl_3 and 1 gram of FeCl_2 in a 25 mL solution of distilled water. Then this solution is heated to 60°C and a drop-wise addition of NaOH was made until the reaction that produced magnetite (Fe_3O_4) (equation 3.1) is done, this happens when the solution turns into black color, the setup is observed in figure 3.3. Subsequently, the solution was left to air cool for 15 minutes. Since the solution had to have a pH between 6.5 and 8 in order to dry in the Stove, it was previously washed using distilled water until the pH was correct. Then the solution was introduced into the stove during 24 hours. With the powder obtained from the dry solution, three distinct samples of magnetite were separated: one at room conditions, while the other two underwent a thermal treatment using the Chemical Vapor Deposition (CVD) apparatus in an Argon environment to change their size, phase, and magnetic properties. The first sample was heated to 250°C and held for 1 hour. Similarly, the second sample was heated to 400°C and held for 1 hour. To reach that temperatures both samples were heated at a rate of 10°C per minute. As a result, three distinct samples of magnetite were synthesized: one at room temperature, one treated at 250°C , and the other treated at 400°C .



3.2.3 Characterization

The techniques used to characterize the magnetite samples were X-ray diffraction (XRD) and Vibrating Sample Magnetometry. The XRD techniques allowed the analysis of the phase composition and nanoparticles size of the magnetite nanoparticles. On the other hand, VSM measurements were performed to determine the magnetic

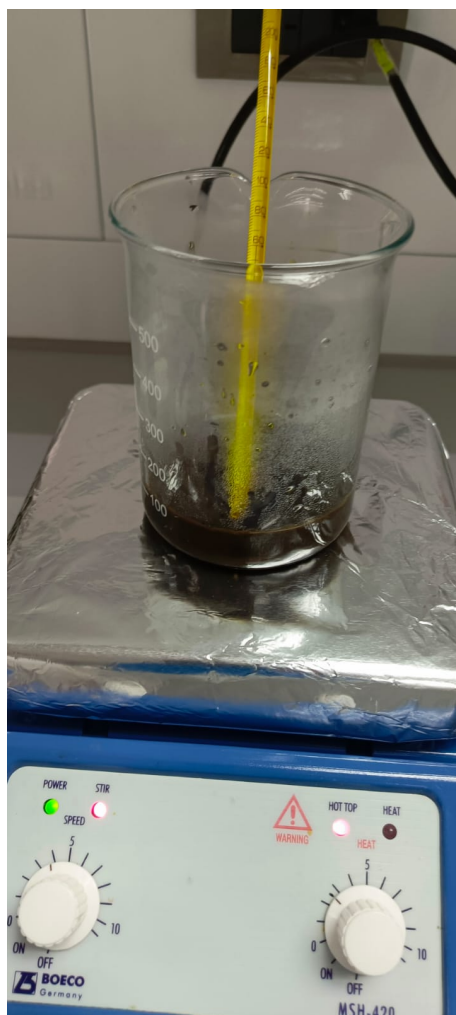


Figure 3.3: Synthesis setup for MNPs

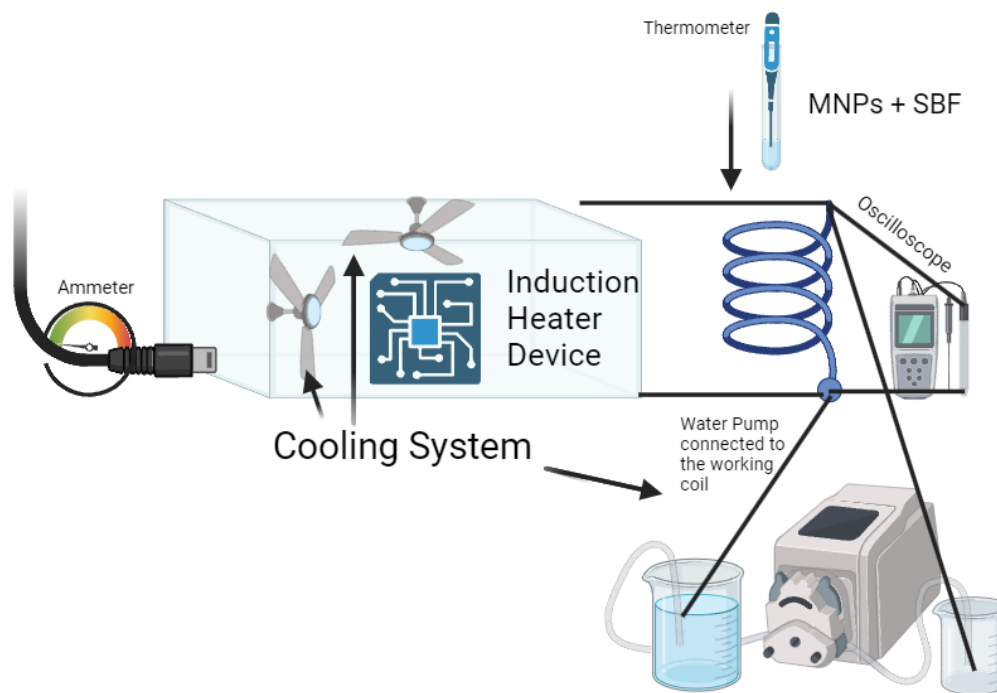


Figure 3.4: Experimental Setup of the Induction Heater and the MNPs

properties of these samples, this data were used to determine the coercivity, remanence and saturation magnetization.

3.3 Validation of the Induction Heating device by using the magnetite nanoparticles

To validate the induction heater with the sample of magnetite nanoparticles, an experimental setup was performed, shown in Figure 3.4. The experimental setup consisted of the induction heater and the magnetite nanoparticles placed inside a test tube with 3 mL of simulated body fluid. The test tube was placed inside the work coil as in Figure 3.4, where an ammeter was used to control the provided current to the power source, an oscilloscope to observe if the device was working correctly, and a thermometer inside the tube to measure the temperature of the sample over time. The temperature readings of the sample were recorded at intervals of one minute. Finally, those data were plotted to be analyzed and compared between the three samples.

Chapter 4

Results & Discussion

4.1 Operation and Functionality of the Induction Heater System

In general, the principal components of the induction heater are the working coil that generates the magnetic field, the transistors that control the flow current through the working coil, and the toroidal inductors are in charge of limiting the current and filtering the electric noise in the circuit (see Figure 3.2), the bank of capacitors and the working coil function as a LC circuit (tank circuit), shown in Figure 4.1, that produce a oscillating circuit. The resonating frequency over time is maintained by turning on and off periodically the Mosfets^{69,70}. When the power supply is turned on, one of the transistors turns on earlier than the other one. When the first MOSFET is on, the gate voltage is high which makes the tank circuit swing up and down. When the circuit is on the way down the diode connected to the gate of the MOSFET drops the gate voltage down, turning it off. This process makes the gate voltage on the second MOSFET increase high enough to turn it on, to produce again the swinging up and down making the cycle continue.

4.2 Induction Heater Device Characteristics

During the construction of the induction heater device, there were some challenges encountered, which included adapting a power supply through a 12V, 4-ampere transformer to power the induction heater system, as depicted in Figure 3.1. Another challenge involved ensuring proper connection of the coil to the capacitor bank's plate, as poor connections led to system failures and increased power consumption, resulting in power supply overheating issues. The temperature control of the equipment was successfully solved by using two fans to cool plate #1 and plate #2, as depicted in Figure 3.1, along with an additional fan for the power supply, also visible in the same Figure. Cooling for plate #3 (see Figure 3.1) only required a cooling system for the working coil since the capacitors did not need additional cooling beyond ambient temperature. Water cooling was employed by connecting a water pump to the coil, allowing water to flow through and cool. The coil cable's hollow nature facilitated this cooling method. It

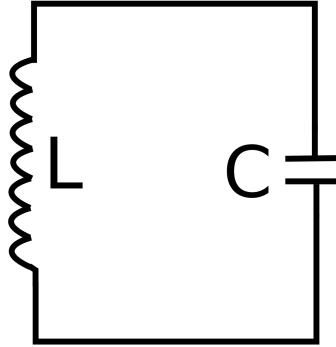


Figure 4.1: LC Circuit (Tank Circuit)

should be noted that even though this device was based on a different model, it was decided not using the two zener diodes that were part of the original design because induction heaters usually don't need them to work.

After the construction of the induction heater shown in Figures 4.2 and 4.3, experimental tests were performed to determine some characteristics of the device. The system shown an alternating current input of 1.31 A, this indicates that the flow of electricity through the system was consistent over time. The direct current voltage measurement was 9.81V after the transformation from alternating current. The experimental oscillation frequency of the induction heater was between 69.9 kHz to 71.1 kHz which is similar to the theoretical value of 77.513 kHz determined by using the equation 2.4. This suggests stable and consistent frequency oscillations during the experimental tests. These results propose that the device can maintain consistent and stable frequency, which are important for applications in hyperthermia therapy. The experimental frequency results indicate that the device operates within the medium frequency range (10 kHz and 70 kHz)²³. Additionally, the value of the magnetic field Even though the heating depends on the properties of the magnetic nanoparticles, the medium frequency range includes advantages such as safer control of current and voltage and minimizes harmful impacts on healthy cells while producing a selective heating effect on cancer cells^{71,72}.

Previous investigations using induction heaters for hyperthermia therapy have examined a range of frequencies and temperature outcomes. In one study, for example, induction heaters for laparoscopic and transrectal procedures were produced. These heaters reached temperatures of 41 °C and 43 °C, respectively, with frequencies of 326 kHz and 303 kHz⁷³. The frequencies used in induction heaters depend on the applications. Induction heaters that use high-frequency waves mainly produce heat in metal samples using frequencies of 250 kHz⁷⁴. Furthermore, a induction heating technique running at 20–30 kHz was created where copper wires were found to be the most effective heating medium⁷⁵.

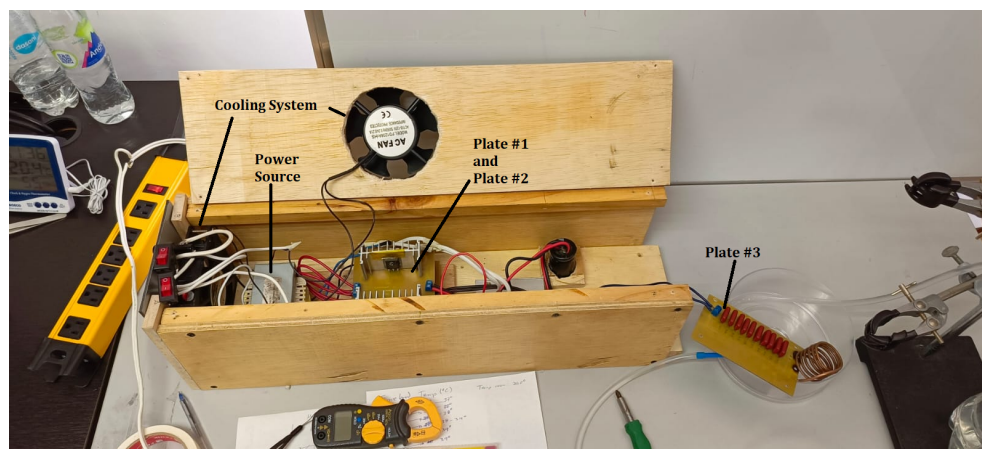


Figure 4.2: Final Setup of the Induction Heater

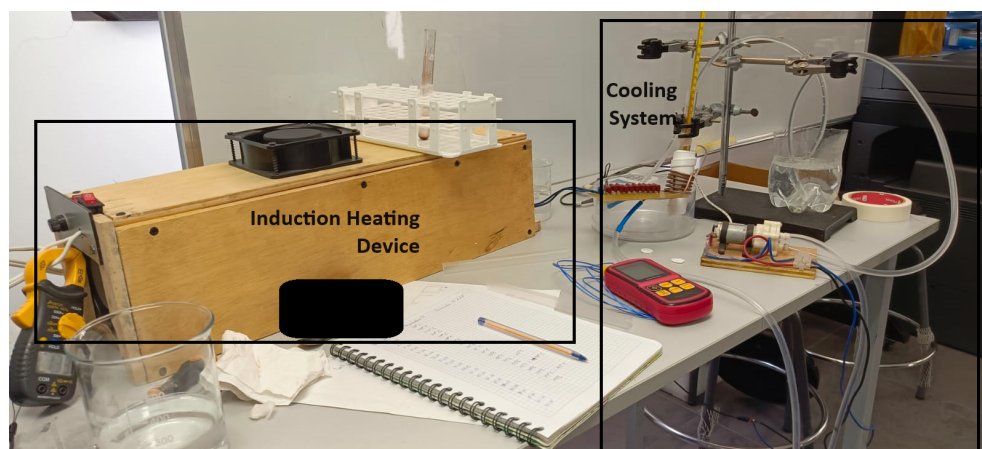


Figure 4.3: Final Setup of the Induction Heater with the Cooling System

4.3 Characterization of Magnetite Nanoparticles

4.3.1 X-rays Diffraction

The Scherrer equation was used to calculate the estimated size of the magnetic nanoparticles. The sample treated at 25°C showed a size of approximately 10.06 nm, which was pretty similar to the MNPs treated at 250°C, that sample had an estimated size of 10.94 nm. Notably, the MNPs held at 400°C for an hour showed significant growth in size with 31.04 nm. This results indicates that changes are not yet noticeable at 250°C. However, at 400°C, the thermal treatment causes significant changes in magnetite nanoparticle size and phase, which are supported by their XRD spectra (Figure 4.4).

Moreover, spectra of the samples treated at 25°C and 250°C showed similarities, according to the analysis done with the QualX software utilizing database cod2205ino. Similar peaks were observed in both spectra, as shown in Figure 4.4 and Figure 4.4, suggesting the presence of magnetite. For these samples, the matching database cards are 00-900-2673 and 00-900-5812 respectively. Furthermore, the lattice parameters were determined to be 8.3851 Å and 8.3778 Å, respectively, based on the database cards. On the other hand, the spectra of the sample that was heated to 400°C showed several peaks associated with the hematite and magnetite phases, which corresponded to phase card 00-210-8027 and 00-900-2673 and similarities with magnetite, as shown in Figure 4.4.

4.3.2 Vibrating Sample Magnetometry

The size of nanoparticles determine their magnetic properties, particularly in terms of remanence, coercivity and maximum magnetization^{76,77}. The hysteresis loop of the samples (Figure 4.5) are summarized in Table 4.1, variations in particle size among the magnetic nanoparticles at different temperatures correspond to notable differences in remanence and coercivity. The size of the MNPs that was previously mentioned as 10.94 nm and 31.04 nm for MNPs treated at 250°C and 400°C, respectively, have their corresponding values of coercivity are 12.981 and 174.659 Oe. In general, higher coercivity is related to an increment in MNPs size⁷⁶. On the other hand, MNPs treated at 25°C and 250°C present similar the same crystalline which is supported by the XRD interpretation that tells it has similar spectra. However, there is a little difference in their remanence and coercivity that is attributed to the magnetic domains ordering when the temperature is increased, as in the 250°C treated sample the magnetic fluctuations decrease and also the magnetic domains walls decrease by temperature⁷⁸. Additionally, the defects decrease with temperature and all of these affect the magnetic properties^{76,78,79}. Moreover, from Figure 4.5 and Table 4.1 can be observed that thermal treatment with higher temperatures can affect the magnetization leading to lower maximum magnetization⁷⁷. In addition, the hysteresis loop for the Magnetite sample treated at 400°C is due to the paramagnetic hematite nanoparticles which have a weak response to magnetic field compared to ferrimagnetic materials such magnetite nanoparticles which have strong response to magnetic^{80,81}.

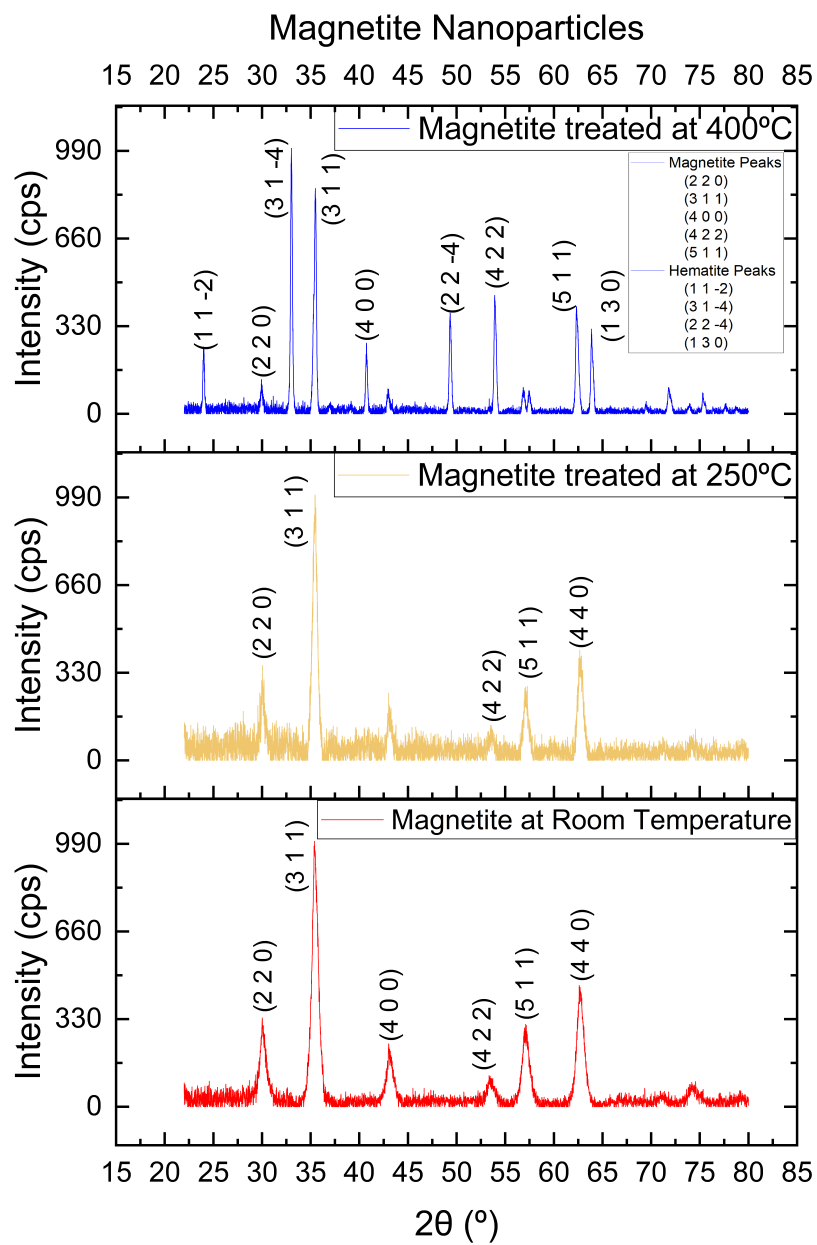


Figure 4.4: Diffraction Spectres of the MNPs treated at different temperatures

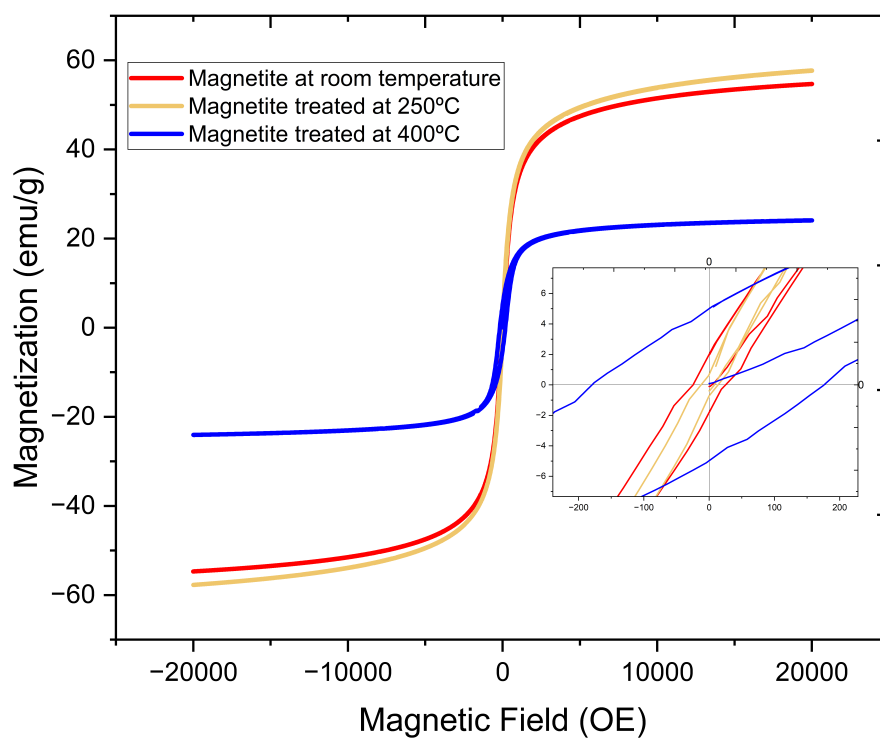


Figure 4.5: Hysteresis loop pattern of MNPs treated ad different temperatures

Sample	Weight (g)	Remanence (emu/g)	Coercivity (Oe)	Maximum Magnetization (emu/g)
25°C	0.0106	1.9073	25.012	54.728
250°C	0.0079	0.70361	12.981	57.799
400°C	0.0076	4.981	174.659	24.086

Table 4.1: Magnetic properties of MNPs treated at different temperatures.

4.4 Validation of the induction heater with the MNPs

After the performance test of temperature vs time, where all three samples of MNPs were under similar conditions and mixed with 3 mL of simulated body fluid (SBF), SBF is a solution commonly used to test the bioactivity of materials simulating the human blood plasma⁸². The Hematite Sample mixed with SBF solution showed a notably different behavior from the magnetite at 25°C and 250°C. In general, the behavior of this sample was unstable reaching a maximum temperature of 38.7°C despite having been subjected to the electromagnetic field produced by the equipment for 2 hours and the minimum temperature of 31.2°C. This behavior is attributed to the hysteresis loop, which has the lowest magnetization behavior due to the superparamagnetic properties of hematite⁸³ (Figure 4.5) compared to the other samples that are ferrimagnetic. Moreover, the data collected (Figure 4.6) for the magnetite samples 25°C and 250°C exhibited similar behavior, as evidenced by their similar temperature-time graphs. The comparable behavior of these samples is evidenced by the similar characteristics observed in both X-rays and hysteresis loop analysis of the two samples. The maximum temperature reached for both magnetite samples 25° and 250°C was 45°C and the starting temperature was 36°C and 37°C starting with an exposition time to the electromagnetic field for 20 min. These results demonstrate the reliability and effectiveness in hyperthermia applications.

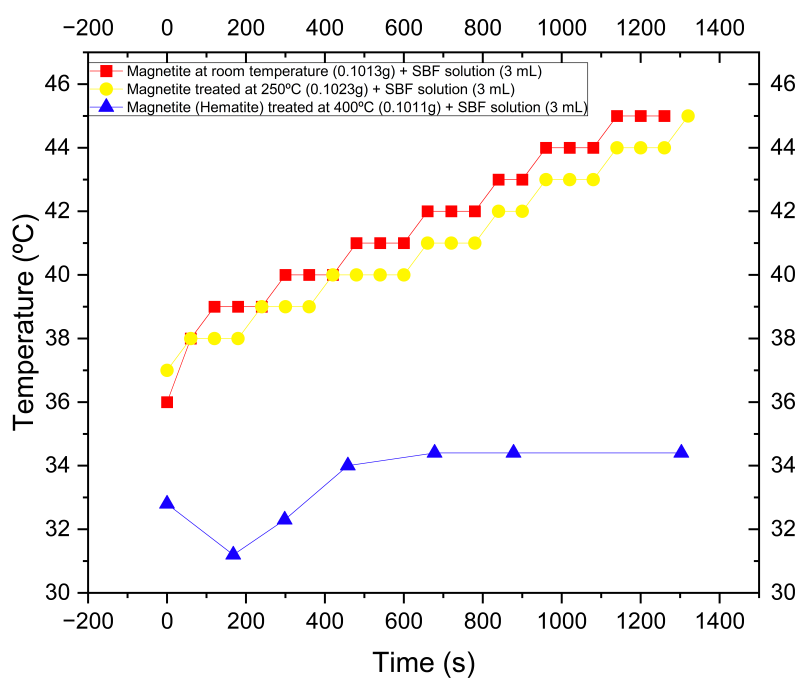


Figure 4.6: MNPs comparison of temperature as a function of time

Chapter 5

Conclusions & Outlook

A homemade device for hyperthermia was built with a very low cost (approximately \$50). The design of the induction heater circuit was designed using the Program PCB Wizard.

The constructed induction heater device shows stable and consistent oscillation frequency, which is relevant for hyperthermia treatment applications.

Magnetic Nanoparticles with different sizes: 10.06, 10.94, 31.04 nm were obtained. The relationship between MNPs size and the temperature achieved under the induction heater device is one of the study's main results. When the device's electromagnetic field was applied to larger MNPs, which were larger with higher coercivity behavior. The smallest particles sized reached higher temperatures when the magnetic field was applied using the device. This finding emphasizes how crucial it is to comprehend how MNPs properties relate to the device's heating capacity to maximize hyperthermia treatments.

Additionally, temperature experiments were performed in conditions similar to those of simulated bodily fluids to simulate near real situations. The hematite sample showed unstable behavior explained by its special magnetic characteristics, but the magnetite samples treated at 25°C and 250°C showed consistent and good temperature responses. This comparison highlights how sensitive the device is to the material and structure of MNPs, highlighting the necessity of accurate temperature control in applications involving hyperthermia.

Overall, the designed induction heating device has great potential for treating hyperthermia since it provides a dependable and efficient way to raise MNPs to therapeutic temperatures. Future research projects can further improve the design and optimization of hyperthermia treatments for in vitro studies involving cancer cell cultures by utilizing the device's capabilities and comprehending the complexity of MNPs interactions.

In an effort to build an induction heating device to achieve the hyperthermia temperature range by using magnetic nanoparticles, this research has shown significant insights about the device's functionality with MNPs of different sizes. Moreover, the experimental results demonstrated the working frequency was in the medium frequency range, which helps select heating in cancer cells without affecting healthy tissues.

The conclusion of this study emphasizes how crucial the induction heating device is to reaching hyperthermia temperatures using MNPs. The device provides a strong platform for advancing hyperthermia therapy through careful

design and characterization, with implications for targeted cancer treatment and enhanced experimental approaches for cancer research.

Bibliography

- [1] Torpy, J. M.; Lynn, C.; Glass, R. M. Cancer: the basics. *Jama* **2010**, *304*, 1628–1628.
- [2] Pérez, A. I. M.; Hernández, I. A.; Hernández, O. B.; Milián, L. S. P. Comportamiento de la mortalidad por tumores malignos. *Medimay* **2011**, *17*, 162–171.
- [3] Manescu, V.; Paltanea, G.; Antoniac, I.; Vasilescu, M. Magnetic nanoparticles used in oncology. *Materials* **2021**, *14*, 5948.
- [4] Rodrigues, D. B.; Dobsicek-Trefna, H.; Curto, S.; Winter, L.; Molitoris, J. K.; Vrba, J.; Vrba, D.; Sumser, K.; Paulides, M. M. *Principles and Technologies for Electromagnetic Energy Based Therapies*; Elsevier, 2022; pp 281–311.
- [5] Kok, H. P.; Crezee, J. Hyperthermia treatment planning: clinical application and ongoing developments. *IEEE Journal of Electromagnetics, RF and Microwaves in Medicine and Biology* **2020**, *5*, 214–222.
- [6] Dedicated 70 MHz RF systems for hyperthermia of challenging tumor locations. *International Journal of Microwave and Wireless Technologies* **2020**,
- [7] Design of a temperature-feedback controlled automated magnetic hyperthermia therapy device. *Frontiers in Thermal Engineering* **2023**,
- [8] Rudnev, V.; Totten, G. E. *Induction heating and heat treatment*; ASM International Materials Park, OH, 2014; Vol. 4.
- [9] Huang, C.-F.; Lin, X.-Z.; Yang, Y.-R. Application of magnetic circuit and multiple-coils array in induction heating for improving localized hyperthermia. *International Journal of Biomedical and Biological Engineering* **2009**, *3*, 305–308.
- [10] Toward the Separation of Different Heating Mechanisms in Magnetic Particle Hyperthermia. *ACS Omega* **2023**,
- [11] Magnetic Nanoparticle Thermometry via Controlled Diffusion. *Particle Particle Systems Characterization* **2022**,

- [12] Xu, Y.; Cui, J.; Puett, D.; Xu, Y.; Cui, J.; Puett, D. Cancer Classification and Molecular Signature Identification. *Cancer Bioinformatics* **2014**, 65–87.
- [13] Abbas, K. Types of Cancer: Carcinoma, Sarcoma, Leukemia, Lymphoma, and Myeloma. 2023; osf.io/tscwp.
- [14] Nainis, N. A. Approaches to art therapy for cancer inpatients: Research and practice considerations. *Art therapy* **2008**, 25, 115–121.
- [15] Symptoms experienced by cancer patients and barriers to symptom management. *Indian Journal of Palliative Care* **2015**,
- [16] A cytokine-based neuroimmunologic mechanism of cancer-related symptoms. *Neuroimmunomodulation* **2003**,
- [17] Magnetic Nanoparticles with Aspects of their Use in Cancer Therapy. *Letters in Drug Design Discovery* **2023**,
- [18] Progressive Study on the Non-thermal Effects of Magnetic Field Therapy in Oncology. *Frontiers in Oncology* **2020**,
- [19] Magnetic Fields and Cancer: Epidemiology, Cellular Biology, and Theranostics. *International Journal of Molecular Sciences* **2022**,
- [20] Behrouzkhia, Z.; Joveini, Z.; Keshavarzi, B.; Eyvazzadeh, N.; Aghdam, R. Z. Hyperthermia: how can it be used? *Oman medical journal* **2016**, 31, 89.
- [21] Kok, H.; Wust, P.; Stauffer, P. R.; Bardati, F.; Van Rhoon, G.; Crezee, J. Current state of the art of regional hyperthermia treatment planning: a review. *Radiation Oncology* **2015**, 10, 1–14.
- [22] Calvo, E. J. Electrochemical methods for sustainable recovery of lithium from natural brines and battery recycling. *Current Opinion in Electrochemistry* **2019**, 15, 102–108.
- [23] Rudnev, V.; Loveless, D.; Cook, R. L. *Handbook of induction heating*; CRC press, 2017.
- [24] Equipment, U. P. T. . I. H. How Induction Heating Works. 2023; <https://ultraflexpower.com/learn-about-induction-heating/induction-heating/#fd55f6f25024b7da6>, 2023.
- [25] Sowa, P.; Rutkowska-Talipska, J.; Sulkowska, U.; Rutkowski, K.; Rutkowski, R. Ionizing and non-ionizing electromagnetic radiation in modern medicine. *Polish Annals of Medicine* **2012**, 19, 134–138.
- [26] Capodaglio, A. G. Critical perspective on advanced treatment processes for water and wastewater: AOPs, ARPs, and AORPs. *Applied Sciences* **2020**, 10, 4549.
- [27] Zhang, H.; Li, H.; Li, W.; Wang, J.; Wang, W.; Zhang, Y.; Teng, L.; Yin, P.; Huang, X. Application of Superparamagnetic Nanoparticle (SPM-NP) Heating in Wax Removal during Crude Oil Pipeline Pigging. *Energies* **2022**, 15, 6464.

- [28] Yang, X.; Feng, Y.; Li, S. Influence of Measuring Coil Geometry on Detection Performance of Eddy Current Sensor. 2018.
- [29] Haerinia, M.; Mosallanejad, A.; Afjei, E. S. Electromagnetic analysis of different geometry of transmitting coils for wireless power transmission applications. *Progress In Electromagnetics Research M* **2016**, *50*, 161.
- [30] Wheeler, H. A. Inductance formulas for circular and square coils. *Proceedings of the IEEE* **1982**, *70*, 1449–1450.
- [31] Alexander, C.; Sadiku, M. *Fundamentos de circuitos eléctricos (5a. ed.)*; 2013.
- [32] Jose, J.; Kumar, R.; Harilal, S.; Mathew, G. E.; Parambi, D. G. T.; Prabhu, A.; Uddin, M. S.; Aleya, L.; Kim, H.; Mathew, B. Magnetic nanoparticles for hyperthermia in cancer treatment: an emerging tool. *Environmental Science and Pollution Research* **2020**, *27*, 19214–19225.
- [33] Fatima, H.; Charinpanitkul, T.; Kim, K.-S. Fundamentals to apply magnetic nanoparticles for hyperthermia therapy. *Nanomaterials* **2021**, *11*, 1203.
- [34] Swagatam, 2 simple induction heater circuits - hot plate cookers. 2021; <https://www.homemade-circuits.com/simple-induction-heater-circuit-hot/>.
- [35] Schematix, 1.4kW induction heater. 2023; <https://www.schematix.co.nz/forum/how-to-s/1-4kw-induction-heater>.
- [36] Biocompatible Iron Oxide Nanoring-Labeled Mesenchymal Stem Cells: An Innovative Magnetothermal Approach for Cell Tracking and Targeted Stroke Therapy. *ACS Nano* **2022**,
- [37] Enhanced magnetothermal effect of high porous bioglass for both bone repair and antitumor therapy. 2023,
- [38] Thermal tissue damage analysis for magnetothermal neuromodulation and lesion size minimization. 2020,
- [39] Rajan, A.; Sahu, N. K. Review on magnetic nanoparticle-mediated hyperthermia for cancer therapy. *Journal of Nanoparticle Research* **2020**, *22*, 1–25.
- [40] Akbarzadeh, A.; Samiei, M.; Davaran, S. Magnetic nanoparticles: preparation, physical properties, and applications in biomedicine. *Nanoscale Research Letters* **2012**, *7*.
- [41] Magnetic Nanoparticles for Therapy and Diagnosis in Nanomedicine. *Pharmaceutics* **2023**, *15*, 1663–1663.
- [42] *Applications and Properties of Magnetic Nanoparticles*; MDPI eBooks, 2023.
- [43] Magnetic Nanoparticles: An Overview for Biomedical Applications. *Magnetochemistry* **2022**, *8*, 107–107.
- [44] Ahmed, S.; Rajak, B. L.; Gogoi, M.; Sarma, H. D. *Smart Healthcare for Disease Diagnosis and Prevention*; Elsevier, 2020; pp 153–173.

- [45] Eddy current effects in the magnetization dynamics of ferromagnetic metal nanoparticles. *arXiv: Mesoscale and Nanoscale Physics* **2014**,
- [46] Pearce, J.; Giustini, A.; Stigliano, R.; Jack Hoopes, P. Magnetic heating of nanoparticles: the importance of particle clustering to achieve therapeutic temperatures. *Journal of nanotechnology in engineering and medicine* **2013**, *4*, 011005.
- [47] Sizing and Eddy currents in magnetic core nanoparticles: an optical extinction approach. *Physical Chemistry Chemical Physics* **2017**,
- [48] The heating efficiency of magnetic nanoparticles under an alternating magnetic field. *Dental science reports* **2022**,
- [49] Specific absorption rate of randomly oriented magnetic nanoparticles in a static magnetic field. *Beilstein Journal of Nanotechnology* **2023**,
- [50] Nano-SAR Modeling for Predicting the Cytotoxicity of Metal Oxide Nanoparticles to PaCa2. *Molecules* **2021**,
- [51] Quantitative Analysis of the Specific Absorption Rate Dependence on the Magnetic Field Strength in Zn x Fe 3x O 4 Nanoparticles. *International Journal of Molecular Sciences* **2020**,
- [52] Threatening sarcoma with combinational therapies: Magnetic hyperthermia using nanoparticles. *Nano select* **2023**, *4*, 353–367.
- [53] Ruiz, A.; Mancebo, A.; Beola, L.; Sosa, I.; Gutiérrez, L. Dose–Response Bioconversion and Toxicity Analysis of Magnetite Nanoparticles. *IEEE Magnetics Letters* **2016**, *7*, 1–5.
- [54] Magnetite Nanoparticles for Biomedical Applications. *Encyclopedia* **2022**, *2*, 1811–1828.
- [55] Effective magnetic hyperthermia induced by mitochondria-targeted nanoparticles modified with triphenylphosphonium-containing phospholipid polymers. *Cancer Science* **2023**,
- [56] Farfán, J. E. S. Síntesis y Caracterización Magneto-Térmica de Nanopartículas de Magnetita y Magnetita Dopada con Zinc. Master's thesis, Universidad Simón Bolívar, Decanato de Estudios de Postgrado, Coordinación de Física, 2016.
- [57] X-ray Diffraction Techniques for Mineral Characterization: A Review for Engineers of the Fundamentals, Applications, and Research Directions. *Minerals* **2022**,
- [58] X-ray Diffraction for the Determination of Residual Stress of Crystalline Material: An Overview. *Transactions of the Indian Institute of Metals* **2022**,
- [59] A Difração de Raios X: uma Técnica de Investigação da Estrutura Cristalina de Materiais. 2020,
- [60] Diffraction Enhanced Imaging Analysis with Pseudo-Voigt Fit Function. *Journal of Imaging* **2022**,

- [61] Retrofittable plug-flow reactor for in situ high-temperature vibrating sample magnetometry with well-controlled gas atmospheres. *Review of Scientific Instruments* **2023**,
- [62] A High Sensitivity Custom-Built Vibrating Sample Magnetometer. *Magnetochemistry* **2022**,
- [63] HYSIGUITS: A MATLAB Graphical User Interface (GUI) for hysteresis loop simulation in Vibrating-Sample Magnetometer (VSM) data. *Journal of physics* **2022**,
- [64] Analysis of Vibrating Sample Magnetometer (VSM) data of Brantas river sediments using HYSITS. *Journal of physics* **2022**,
- [65] Electrical4U, Hysteresis Loop: What is it (and what is its significance)? 2021; <https://www.electrical4u.com/hysteresis-loop/>.
- [66] Admin, Live wire Y PCB wizard Para Diseño Electrónico . 2021; <https://electronicabasica.site/live-wire-y-pcb-wizard/>.
- [67] tannertech, DIY induction heater. 2017; <https://www.instructables.com/DIY-Induction-Heater/>.
- [68] Berger, P.; Adelman, N. B.; Beckman, K. J.; Campbell, D. J.; Ellis, A. B.; Lisensky, G. C. Preparation and properties of an aqueous ferrofluid. *Journal of chemical education* **1999**, 76, 943.
- [69] Exploitation of MOSFET based AC switches in capacitive impedance matching networks in inductive wireless power transfer systems. *Iet Power Electronics* **2020**,
- [70] Modelling and Controlling of Induction Heating Unit for Induction Cooking Application. 2020,
- [71] Induction Heating of Magnetic Fluids for Hyperthermia Treatment. *IEEE Transactions on Magnetics* **2010**,
- [72] Development of handheld induction heaters for magnetic fluid hyperthermia applications and in-vitro evaluation on ovarian and prostate cancer cell lines. *Biomedical Physics Engineering Express* **2023**,
- [73] Development of handheld induction heaters for magnetic fluid hyperthermia applications and in-vitro evaluation on ovarian and prostate cancer cell lines. *Biomedical Physics Engineering Express* **2023**,
- [74] Development of a high frequency Induction Heater and related temperature monitoring system. 2020,
- [75] VLF induction heating for clinical hyperthermia. *IEEE Transactions on Magnetics* **1986**,
- [76] Coercivity of magnetic nanoparticles: a stochastic model. *Journal of Physics: Condensed Matter* **2007**,
- [77] Diamagnetic-like response from localized heating of a paramagnetic material. *Applied Physics Letters* **2020**,
- [78] Pasko, A.; Pecheux, A.; Tyrman, M.; Perrière, L.; Guillot, I.; Etgens, V.; Lobue, M.; Mazaleyrat, F. Temperature dependence of coercivity and magnetic relaxation in a Mn–Al–C permanent magnet. *IEEE Transactions on Magnetics* **2020**, 57, 1–5.

- [79] Kechrakos, D.; Trohidou, K. Magnetic properties of dipolar interacting single-domain particles. *Physical Review B* **1998**, *58*, 12169.
- [80] Terahertz Spin Current Dynamics in Antiferromagnetic Hematite. *Advanced Science* **2023**,
- [81] Magnetite-like mixed-valence iron ferrimagnetic homohelical chains exhibiting spin canting, spin-flop and field induced SCM like behaviours. *Inorganic chemistry frontiers* **2019**,
- [82] Role of Simulated Body Fluid in Biofilm Formation and Growth on a Polycarbonate Material. *Key Engineering Materials* **2022**,
- [83] Tadic, M.; Panjan, M.; Damnjanovic, V.; Milosevic, I. Magnetic properties of hematite (α -Fe₂O₃) nanoparticles prepared by hydrothermal synthesis method. *Applied Surface Science* **2014**, *320*, 183–187.